

Clinical Medicine Insights: Oncology

Impact of Andrographolide and Melatonin Combinatorial Drug Therapy on Metastatic Colon Cancer Cells and Organoids

Journal:	<i>Clinical Medicine Insights: Oncology</i>
Manuscript ID	ONC-20-0135.R1
Manuscript Type:	Original Research Article
Date Submitted by the Author:	n/a
Complete List of Authors:	Sharda, Neha; University of Maryland School of Medicine, Pediatrics Ikuse, Tamaki; Juntendo University School of Medicine Graduate School of Medicine Department of Anesthesiology Pain Clinic, Department of Pediatric and Adolescent Medicine, Hill, Elizabeth; University of Maryland School of Medicine Garcia, Sonia; University of Maryland School of Medicine, Pediatrics Czinn, Steven; University of Maryland School of Medicine, Pediatrics Bafford, Andrea; University of Maryland School of Medicine, Surgery Blanchard, Thomas; University of Maryland School of Medicine, Pediatrics Banerjee, Aditi; University of Maryland School of Medicine, Pediatrics
Keywords:	Apoptosis, Colorectal cancer, Metastasis, Chemotherapy, Complementary medicine
Abstract:	<p>Background: The death rate (the number of deaths per 100,000 people per year) of colorectal cancer (CRC) has been dropping since 1980 due to increased screening, lifestyle-related risk factors, and improved treatment options; however, CRC is the third leading cause of cancer-related deaths in men and women in the US. Therefore, successful therapy for CRC is an unmet clinical need. The present study aimed to investigate the impacts of andrographolide (AGP) and melatonin (MLT) on CRC and the underlying mechanism.</p> <p>Methods: To investigate AGP and MLT anticancer effects, a series of metastatic colon cancer cell lines (T84, Colo 205, HT-29, and DLD-1) were selected. In addition, a metastatic patient-derived organoid model (PDOD) was used to monitor the anti-cancer effects of AGP and MLT. A series of bioassays including 3D organoid cell culture, MTT, colony formation, western blotting, immunofluorescence, and qPCR were performed.</p> <p>Results: The dual therapy significantly promotes CRC cell death, as compared with the normal cells. It also limits CRC colony formation and disrupts the PDOD membrane integrity along with decreased Ki-67 expression. A significantly higher cleaved caspase-3 and the endoplasmic reticulum (ER) stress proteins, IRE-1 and ATF-6 expression, by 48 h were found. This combinatorial treatment increased ROS levels. Apoptosis signaling molecules BAX, XBP-1, and CHOP were significantly increased as determined by qPCR.</p> <p>Conclusions: These findings indicated that AGP and MLT associated ER</p>

1
2
3
4
5
6
7
8
9
10
11
12
13
14
15
16
17
18
19
20
21
22
23
24
25
26
27
28
29
30
31
32
33
34
35
36
37
38
39
40
41
42
43
44
45
46
47
48
49
50
51
52
53
54
55
56
57
58
59
60

	stress-mediated apoptotic mCRC cell death through the IRE-1/XBP-1/CHOP signaling pathway. This novel combination could be a potential therapeutic strategy for mCRC.



Impact of Andrographolide and Melatonin Combinatorial Drug Therapy on Metastatic Colon Cancer

Neha Sharda¹, Tamaki Ikuse^{1&2}, Elizabeth Hill¹, Sonia Garcia¹, Steven J. Czinn¹, Andrea Bafford³, Thomas G. Blanchard¹, Aditi Banerjee^{1*}.

¹Department of Pediatrics, University of Maryland School of Medicine, Baltimore, Maryland, U.S.A., ² Department of Pediatric and Adolescent Medicine, Juntendo University Graduate School of Medicine, Tokyo, Japan, ³ Department of Surgery, University of Maryland School of Medicine, Baltimore, MD, U.S.A.

*Corresponding author

Department of Pediatrics,
University of Maryland School of Medicine,
Bressler Research Building, 13-043,
655 W. Baltimore Street, Baltimore, MD 21201,
Voice: (410) 706-1772, Fax: (410) 328-1072, Email: aditi.banerjee@som.umaryland.edu

Running Title: Impact of combinatorial drug on metastatic colon cancer

Keywords: Andrographolide, Melatonin, Metastatic colon cancer, Endoplasmic reticulum stress, Reactive oxygen species, patient-derived organoids.

**Impact of Andrographolide and Melatonin Combinatorial Drug Therapy on Metastatic
Colon Cancer Cells and Organoids**

For Peer Review

1 Abstract

2 **Background:** The death rate (the number of deaths per 100,000 people per year) of colorectal
3 cancer (CRC) has been dropping since 1980 due to increased screening, lifestyle-related risk
4 factors, and improved treatment options; however, CRC is the third leading cause of cancer-related
5 deaths in men and women in the US. Therefore, successful therapy for CRC is an unmet clinical
6 need. The present study aimed to investigate the impacts of andrographolide (AGP) and melatonin
7 (MLT) on CRC and the underlying mechanism.

8 **Methods:** To investigate AGP and MLT anticancer effects, a series of metastatic colon cancer cell
9 lines (T84, Colo 205, HT-29, and DLD-1) were selected. In addition, a metastatic patient-derived
10 organoid model (PDOD) was used to monitor the anti-cancer effects of AGP and MLT. A series
11 of bioassays including 3D organoid cell culture, MTT, colony formation, western blotting,
12 immunofluorescence, and qPCR were performed.

13 **Results:** The dual therapy significantly promotes CRC cell death, as compared with the normal
14 cells. It also limits CRC colony formation and disrupts the PDOD membrane integrity along with
15 decreased Ki-67 expression. A significantly higher cleaved caspase-3 and the endoplasmic
16 reticulum (ER) stress proteins, IRE-1 and ATF-6 expression, by 48 h were found. This
17 combinatorial treatment increased ROS levels. Apoptosis signaling molecules BAX, XBP-1, and
18 CHOP were significantly increased as determined by qPCR.

19 **Conclusions:** These findings indicated that AGP and MLT associated ER stress-mediated
20 apoptotic mCRC cell death through the IRE-1/XBP-1/CHOP signaling pathway. This novel
21 combination could be a potential therapeutic strategy for mCRC cells.

1 2 3 4 5 6 7 8 9 10 11 12 13 14 15 16 17 18 19 20 21 22 23 24 25 26 27 28 29 30 31 32 33 34 35 36 37 38 39 40 41 42 43 44 45 46 47 48 49 50 51 52 53 54 55 56 57 58 59 60

1 Introduction

2 The American Cancer Society (ACS) estimates that, in 2020 alone, there will be 104,610 new
3 diagnoses of colon cancer in the United States. The majority of CRCs occur in adults ages 50 and
4 older, 17,930 (12%) of cases are diagnosed in individuals younger than age 50, the equivalent of
5 49 new cases per day ¹. Chemotherapy, targeted therapy, and immunotherapy are the current
6 treatment options for CRC, though each strategy has its own limitations ²⁻⁴. Therefore, targeting
7 mCRC **cells** via molecular targets remain important in colon cancer therapy.

8 **Combination therapy, a treatment modality which combines two or more therapeutic**
9 **agents, is a cornerstone of cancer therapy ^{5,6}. Moreover, this therapy is a promising strategy for**
10 **synergistic anticancer treatment. It has different mechanisms of action that could reduce the dose**
11 **of each agent, thus may reduce the individual drug-related toxicity ⁶. The studies carried out if two**
12 **combinatorial drug has an impact of metastatic colon cancer cells and stage III patient-derived**
13 **organoids. Earlier** studies have demonstrated that the plant metabolite andrographolide (AGP)
14 induces CRC cell death due to apoptosis and is associated with the activation of IRE-1, an ER
15 stress marker ⁷. Additional studies showed that AGP induces apoptotic cell death through the
16 induction of reactive oxygen species (ROS) which eventually play a role in down-regulating cell
17 cycle progression and cell survival pathways ⁸. AGP also induces cell death through the inhibition
18 of angiogenic signaling, which is inversely related to the tumor suppressor gene expression,
19 RASSF1A ⁹. Co-treatment of AGP with other substances suggests its potential in combination
20 therapies. In the context of cancer, AGP can diminish resistance to 5-Fluorouracil (5-FU), a first-
21 line chemotherapeutic agent for CRC patients ^{10,11}.

22 Recent studies have also shown that melatonin (MLT) has antimetastatic properties by
23 modulating cell-cell and cell-matrix interactions, remodeling the extracellular matrix, and

suppressing angiogenesis¹²⁻¹⁴. In addition, extensive experimental data demonstrates that this chronobiotic agent exerts oncostatic effects throughout all stages of tumor growth, from initial cell transformation to mitigation of malignant progression and metastasis; additionally, MLT alleviates the side effects and improves the welfare of radio/chemotherapy-treated patients¹⁵. Moreover, it inhibits CRC proliferation by increasing reactive oxygen species (ROS) and inducing apoptosis, autophagy, and senescence¹⁶. Additionally, MLT also causes drug-resistant CRC cell death and inhibits CRC-colospheroids when it is co-administered with 5-FU¹⁷. In the present study, we tested the potential of AGP to inhibit CRC cell growth with reduced concentration compared to prior studies when combined with the safe, anti-cancer compound MLT. We demonstrate this dual compound has an impact on metastatic CRC cells (T84, Colo 205, HCT-15, HT-29, and DLD-1), and requires a concentration 3 times less than in previous studies. Moreover, these combinatorial therapies exert a little impact on normal cells.

Methods

Ethics Statement

All de-identified metastatic colon cancer tissues were received from the surgery of colon cancer patients with the approval the University of Maryland Institutional Review Board (HP-00066889-4). Written consent was obtained from all patients from whom discarded tissue was collected which included permission to publish results. A small piece of each tumor tissue was frozen for subsequent analysis and remaining tissue was processed for organoid cultures.

Generation and Propagation of Patient-Derived Organoid Cell Cultures (PDOD)

1 Organoid cells were generated from stage 3 metastatic cancer tissue and cultured as previously
2 described ^{9,18,19}. The cultures were passaged when the aggregates reached a diameter of
3 approximately 800 μ m. Organoids were treated with 15 μ M AGP, 0.5 mM MLT, or both for 48 h.
4 Treated and untreated organoids were subjected to morphological analysis and
5 immunofluorescence for Ki67 expression.

6 *Cell Culture and Drug treatment*

7 T84, and Colo 205 colon cancer cell lines were cultured as previously published ^{7-9,19}. HT-29, and
8 DLD-1 were grown in RPMI-1640 nutrient media in a humidified incubator at 37°C with 5% CO₂.
9 All media were supplemented with a 1X solution of antimicrobial reagents (10,000 U/ml penicillin,
10 10,000 streptomycin, and 25 μ g/ml amphotericin B), 1X glutamine and 10% FBS. Mouse normal
11 epithelial cells (GSM06) and prostate epithelial cells (RWPE1) cells were grown and cultured as
12 previously described ¹⁹. When cell was grown 80% confluent, media was replaced with media
13 containing 2% FBS with AGP (Sigma Aldrich, St. Louis, MO) and MLT (a kind gift from
14 Professor Russel J. Reiter) with indicated dose and time point. Stock AGP (100 mM) and MLT (1
15 M) were prepared in DMSO and control wells received DMSO at a final concentration of 0.01%.

17 *Cytotoxicity Assay*

18 Cytotoxicity assay in the presence or absence of AGP or, MLT was assessed using the MTT assay
19 as previously described ⁷.

20 *Clonogenic Assay*

HT-29 and DLD-1 cells were seeded in 6-well plates (approximately 50,000/well). The clonogenic assay was performed as previously described ⁷.

Quantitative real-time polymerase chain reaction (qRT-PCR)

Gene expression was evaluated as previously described ⁷. Primer sequences are listed in Supplementary Table 1. Relative gene expression changes were calculated using the $2^{-\Delta\Delta CT}$ method and expression normalization was accomplished using the housekeeping gene, GAPDH.

Immunoblotting

Immunoblotting was performed as previously described ²⁰. The primary antibodies used were against Cleaved caspase-3 (#MAB835) from R&D Systems, Caspase 3 (#9662), IRE-1(#3294) from Cell Signaling, Cyclin B1(GNS1, #sc-245), p-PERK (#sc-32577), PRX (A-6) (#sc-137150P), TRX (#sc-271281) from Santa Cruz Biotechnology, ATF-6 (#MA5-16172) from Thermo Fisher Scientific, melatonin receptor 1B or MT2 (#NLS9320 from Novus Biologicals and GAPDH (G8795) from Sigma Aldrich. Blots were incubated with HRP-conjugated secondary antibodies followed by enhanced chemiluminescence (ECL) detection. All secondary antibodies were purchased from KPL, Gaithersburg, MD. Images were captured using a Syngene G Box digital imager (Frederick, MD, USA) and results were quantified by densitometry as previously described ¹⁹.

Immunofluorescence

Patient derived organoids were grown in 1:1 mixture of Matrigel and advanced DMEM:F12 (Life Technologies) supplemented with 1X penicillin/streptomycin, 1x glutamine, 1X N2, 1X B27, 1mM N-acetyl-L-cysteine, 20 ng/ml fibroblast growth factor and 50 ng/ml epidermal growth factor at 37°C on a 4-chambered glass slide. Fully grown organoids were treated with or without AGP

1 and MLT for 48 h. whole mount staining was carried out as previously described ^{9,21} with slight
2 modifications. After desired time of treatment organoids were washed three times with 1X PBS
3 and fixed with 4% paraformaldehyde at room temperature for 30 min, permeabilized with 0.2%
4 Triton X-100 for 20 min, blocked with 2.5% horse serum (Vector; S-2012) and incubated with
5 1:40 dilution of Ki-67 (M-19) (#sc-7846) at 4°C for overnight. After incubation organoids were
6 washed 3 times with PBS (10 mins/wash) and incubated with Alexa Flour 488 labeled donkey
7 anti-goat IgG (H+L) (1:200) (ab 150129).

8 *Fluorescence microscopy and image acquisition*

9 Fluorescence microscopy and colony counting were performed using an inverted fluorescence
10 microscope (Olympus IX-71, Pennsylvania, USA). Images for patient derived organoids (PDOD)
11 were taken at 400 X magnification. Fluorescence intensity was quantified using ImageJ software
12 version 1.39 (NIH). RGB composite images from control and treated groups were created using
13 Axion Vision rel, 4.6 and analyzed. Images from five different fields were used for statistical
14 analysis as previously described ^{8,9,21}.

16 *Statistical Analysis*

17 Statistical analysis was performed with Graph Pad Prism for Macintosh 5.0c (Graph Pad Software
18 Inc., San Diego, CA). The mean S.E. was calculated by one-way ANOVA. Significance between
19 groups was analyzed using the post hoc Tukey's test and Bonferroni test. A p<0.05 was considered
20 statistically significant.

23 **Results**

24 *Co-treatment with AGP and MLT inhibits cell viability*

Previous study have demonstrated that the IC_{50} value of AGP for T84 and Colo 205 is $45 \mu M$ ⁷, whereas IC_{50} value of MLT for CRC range from 1-2.5 mM^{22,23}. To reduce the AGP concentration, T84, Colo 205, HT-29 and DLD-1 cells were co-treated with AGP (0-150 μM) and MLT (0.5 mM) for 24, 48 and 72 h to assess the effect on cell proliferation. MTT assays revealed co-treatment significantly reduced cell viability in a time and dose dependent manner (Fig. 1A-D). The IC_{50} was determined to be 15 μM for AGP and 0.5 mM for MLT at 48 h. This concentration was used for subsequent assays. Additional experiments were performed to determine the efficacy of this co-treatment on normal cells such as gastric surface mucous cell lines from transgenic mice GSM06 and normal prostate epithelial cells (RWPE-1). Co-treatment of normal epithelial cells with the same concentration of AGP and MLT had little effect on cell numbers (Fig. 1E-F). These data suggest that AGP and MLT co-treatment selectively inhibits CRC cells but not normal cells. The inhibitory properties of AGP and MLT on HT-29 and DLD-1 cells were also determined in a clonogenic assay and direct enumeration of stained colonies (Fig. 2). Co-treatment of cells for 48 h resulted in significantly fewer colonies compared with the untreated cells. Co-treatment significantly decreased the number of colonies ($P < 0.001$) by 48 h.

Co-treatment with AGP and MLT induces apoptosis and apoptosis signaling is dependent upon ER stress

Earlier studies showed that AGP, at a concentration of $45 \mu M$, causes apoptotic CRC cell death due to the unfolded protein response (UPR) mediated ER stress pathway⁷⁻⁹. To verify the function of a lower concentration of AGP on CRC cells, T84 and Colo 205 cells were co-treated with AGP and MLT as indicated. As shown in Figure 3A and 3B, co-treatment significantly increased the 17kDa cleaved Caspase 3 levels ($P < 0.001$) as compared with the control and treatment with either AGP or MLT alone. The ratio of cleaved caspase 3 and total caspase 3 also significantly increased

(Fig. 3C; $P<0.001$). Additionally, co-treatment significantly upregulated pro-apoptotic BAX mRNA expression (Fig. 3D; $P<0.001$), but not mRNA of Bcl-2 (Fig. 3E T84). To verify the apoptotic induction with co-treatment of AGP and MLT is due to the *UPR*, T84 and Colo 205 mRNA levels were monitored for *UPR* signaling pathway initiators IRE-1, ATF-6 and PERK. Co-treatment resulted in a significant increase in IRE-1 and ATF-6 mRNA expression (~4.5-6-fold, $P<0.001$) at 48 h (Fig. 4A, B). Consistent with IRE-1 activation, an increase in XBP-1 mRNA expression of over 3.5-fold for T84 and 1.5-fold for Colo 205 was observed at 48 h (Fig. 4C; $P<0.001$ and $P<0.05$). Expression of CHOP, which can be activated by XBP-1, was also significantly increased (Fig. 4D; $P<0.05$ for T84 and $P<0.01$ for Colo 205). An additional experiment was performed to monitor the ER stress protein level (IRE-1, p-PERK, and ATF-6) by western blot. ER stress protein analysis revealed increases only in IRE-1 in T84 and Colo 205 co-treated groups and ATF-6 expression in T84 co-treated group (Fig. 4E, F, and H). Taken together, the results indicate that co-treatment induced apoptosis is mediated via ER stress and the IRE-1 activation pathway.

Co-treatment induced G2/M cell cycle arrest and involvement of ROS molecules. AGP alone suppresses Cyclin B1 expression in T84 and Colo 205 cell lysates ⁸. To monitor the Cyclin B1 expression in co-treatment groups, T84 and Colo 205 cells were treated with or without AGP and MLT. The cell lysates were analyzed for Cyclin B1 expression. Fig. 5A and 5A1 show AGP and MLT could effectively suppress Cyclin B1 expression ($P<0.001$) as compared to untreated control and AGP or MLT alone groups. Next, we monitored antioxidant protein expression (Prx, and Trx) by western blot. Peroxiredoxin (Prx) and Thioredoxin-1 (Trx-1) are upregulated in many human

cancers, including colon and rectum, and in some cancers, downregulation of Prx promotes apoptosis²⁴⁻²⁶.

Our findings indicate co-treatment significantly downregulates Prx and Trx expression (Fig. 5B-B1; $P<0.05$ - $P<0.001$) in both cell lysates. Taken together, the results depicted that co-treatment causes cell cycle arrest through downregulation of cyclin B1 and Prx- and Trx- mediated oxidative stress-induced cell apoptosis.

Impact of AGP and MLT on patient derived organoids

Patient derived organoids were generated as previously described⁹ (Fig. 6A). Matured organoids were treated with or without AGP (15 μ M) and MLT (0.5 mM) for 48 h. A loss of membrane integrity was found in the co-treatment group as compared with the AGP or MLT alone groups. Untreated group retained the structure of 3D organoids with intact membrane integrity (Fig. 6B). Immunofluorescence staining for Ki-67 expression was evaluated to measure the effect of AGP, MLT or co-treatment of AGP and MLT on organoids growth. Ki-67 was greatly reduced in all treatment groups as compared to the untreated group; maximum reduction was found in the co-treatment group (Fig. 6C).

Discussion

Colorectal cancer is the third most prevalent malignant tumor worldwide and the number of new cases may increase to nearly 2.5 million in 2035^{27,28}. The 5-year survival rate for CRC is ~64%, but drops to 12% for metastatic CRC, and therefore, additional treatment regimens are needed to develop effective approaches for medical intervention²⁹.

Previous studies have demonstrated that AGP alone causes inhibition of CRC cell proliferation in metastatic cell lines, and patient derived organoids at a concentration of 45 μ M. The inhibition was shown to be due to ER stress mediated apoptosis ⁷⁻⁹. Moreover, AGP displayed synergistic effect with chemotherapeutic drugs in CRC cells and hepatocellular carcinoma cells ^{30,31}. *In vitro and in vivo* studies have demonstrated the significant role AGP can have in re-sensitizing 5-Fu-resistant HCT116 (HCT116/5-FuR) cells to the cytotoxic effects of 5-Fu. AGP reverses 5-Fu resistance in human CRC through increasing the expression of BAX ¹¹. AGP, either alone or in combination with cisplatin, also induces CRC apoptotic cell death via increasing the expression of BAX and Bcl-2 and increasing the association of Fas and FasL ³². Additional study provided the evidence its possible clinical application for enhancing the antitumor effort ³³. Recently, it is reported the synergistic cytotoxicity of AGP and MLT in mCRC cell lines, colospheroids and 5-FU drug resistance cells ³⁴ and the molecular mechanism is apoptosis due to unfolded protein response mediated ER stress and angiogenic inhibition. In the present study, we have used a combination of AGP and MLT for metastatic CRC cell inhibition as both compounds have anti-angiogenic, apoptotic, cell cycle arrest dysregulation of various cancer signaling pathways and involved in regulation of immune function and tumor microenvironments ³⁴. Here, we examined the uses of a lower concentration of AGP when administered in combination with MLT (0.5 mM). The therapeutic concentration of MLT (0.5 mM) was selected because it modulates several signaling pathways which are considered likely anti-metastasis, anti-proliferative, and pro-apoptotic pathways in cancer cells ^{13,17,23,35,36}. Moreover, MLT does not show undesired side effects, even at extremely high doses ^{37,38}. However, on pharmacological grounds, MLT can be designated as a synergistic or potentiating effect and it may have a potential clinical implication in the treatment of several pathologies including neurodegenerative diseases ³⁹

1 Additionally, it inhibits CRC stem cells by regulating the PrP^c-Oct4 axis. A synergistic effect has
2 also been observed with MLT when combined with 5-Fu by inhibiting the stem cell markers Oct4,
3 Nanog, Sox2 and ALDH1A1 through regulation of PrP^c ¹⁷.

4 We screened the potential effect of an AGP and MLT co-treatment on a panel of CRC cells
5 and normal cells. The IC₅₀ value of AGP in co-treatment is reduced 3-fold compared with AGP
6 alone ^{7,8}. Co-treatment of AGP and MLT inhibits cell viability and has significantly less
7 cytotoxicity in mouse normal epithelial cells and human prostate epithelial cells. Co-treatment
8 induces an increase in mRNA and protein levels of IRE-1, one of the three major ER stress
9 activated UPR proteins; an observation that is consistent between two cell lines. Increases in
10 transcription of ATF6 mRNA were observed in T84 and Colo 205 cells, but protein levels only
11 increased in T84 cell lysates at 48 h. Therefore, involvement of UPR protein at 48 h is associated
12 with an increase in pro-apoptotic signaling and cell death.

13 Reactive oxygen species (ROS) generation can induce carcinogenesis by stimulating
14 mutation and can inhibit tumor progression by inducing apoptotic signals ⁴⁰. Studies have
15 demonstrated the importance of ROS in AGP-induced anti-cancer cell activities ⁸. Among the Prx
16 family of proteins, Prx-1 is the most prominent subtype with an increase in expression in tumor
17 tissues ⁴¹. Trx-1, a small redox protein, also has shown an increase in expression when observed
18 in many human cancers including colon cancer. We have observed that co-treatment
19 downregulates Prx-1 and Trx expression, which is consistent with the elevated expression of
20 cleaved caspase 3, CHOP, and XBP-1 and the decreased expression of Cyclin B1.

21 Patient derived models are necessary to improve knowledge about CRC and to develop new
22 therapeutic approaches. Our model represents an informative system employing both *in vitro* and
23 *ex vivo* testing, support by a previous study ⁴². Our data show the impact of AGP and MLT on the

inhibition of organoid morphology derived from third metastatic CRC patient tissue, which corroborates the inhibition of Ki67. A significant amount of Ki67 in organoids in the untreated group is consistent with another study which reports elevated Ki67 in CD133⁺, CD44⁺/CD24⁻ and ALDH⁺ CSCs ⁴³. Multiple studies have demonstrated that besides having a role in cell proliferation, Ki67 is also involved in metastasis and invasion of cancer cells ^{43,44}. These studies support a role for dual therapy using the natural products AGP and MLT against CRC.

Conclusion

This is the first report analyzing the potential of dual AGP and MLT treatment on CRC using CRC cell lines as well as patient-derived CRC organoids. The dual treatment was demonstrated to inhibit cell viability and promote cell cycle arrest as well as promote ER stress dependent apoptosis signaling in CRC cell lines. Cancer organoids derived from metastatic CRC were also shown to display membrane disruption and reduced proliferative activity in response to AGP and MLT treatment compared to control organoids. The molecular mechanisms that contribute to cell death in CRC cells in response to AGP and MLT remain unclear. Therefore, further investigation on this combination therapy will be necessary to delineate the molecular interactions within the CRC PDOD model.

Figure Legends

Figure 1. Impact of AGP and MLT on mCRC cell viability. A. T84, B. Colo 205, C. HT-29, D. DLD-1 E. GSM06 (gastric surface mice mucous), and F. RWPE-1 (prostate epithelial cells were

1 treated with indicated concentration of AGP (0-150 μ M), and MLT (0.5 mM) for 24 h, 48 h, and
2 72 h. Cell viability was quantified using the MTT assay.

3
4 Figure 2. Co-treatment suppress clonogenicity in HT-29 and DLD-1 cells. HT-29 and DLD-1 cells
5 were diluted and treated with AGP and MLT as indicated dose. Growth was measured by direct
6 counting of clonal clusters stained in multiwell plates with crystal violet at 48 h. Representative
7 micrographs are shown.

8 Figure 3. Co-treatment of AGP and MLT induced cell apoptosis. T84 and Colo 205 cells were
9 treated with or without AGP and MLT at IC₅₀ for 48 h and protein expression was determined by
10 immunoblotting for Cleaved caspase 3 (A, upper lane), Caspase 3 (A, middle lane) and GAPDH
11 (A, lower lane). Densitometry analysis was performed and normalized with GAPDH expression
12 to determine significant upregulation of indicated proteins (Fig. 3B and 3C). The mRNA level
13 for apoptosis associated genes was determined by qRT-PCR for BAX (D), Bcl-2 (E). Bar graphs
14 show quantitative results normalized to GAPDH mRNA levels. Results are from three
15 independent experiments. Statistical significance was determined using one way-ANOVA
16 followed by Bonferroni test (*P<0.05, **P<0.01, ***P<0.001).

17 Figure 4. AGP and MLT induces ER stress-related IRE-1 and associated proteins. T84 and Colo
18 205 cells were treated as mentioned earlier. The transcriptional level of expression for ER stress
19 associated genes was determined by qRT-PCR for A. IRE-1, B. ATF-6, C. XBP-1 and D. CHOP.
20 Bar graphs show quantitative results normalized to GAPDH mRNA levels. The primary ER
21 transducer translational level was determined by immunoblotting for E. IRE-1 (level 1), p-PERK
22 (level-2), and ATF-6 (level-3). Densitometry analysis was performed and normalized with
23 GAPDH (blot 4). Results are from three independent experiments. Statistical significance was

determined using one way- ANOVA followed by Bonferroni test. (*P<0.05, **P<0.01, ***P<0.001).

Figure 5. Co-treatment induced cell cycle arrest and decreased antioxidant protein expression in CRC cells. T84 and Colo 205 cells were treated with or without AGP (15 μ M) and MEL (0.5 mM) for 48 h. Cell lysates were analyzed by immunoblot for cyclin B1 (A), PRX (B, upper lane), and TRX (B, middle lane) and quantified by densitometry for expression of A1. Cyclin B1, B1 (left) PRX and (right) TRX. Expression is normalized against GAPDH expression. Statistical significance was determined using one way-ANOVA followed by Bonferroni test (*P<0.05, **P<0.01, ***P<0.001).

Figure 6. Impact of AGP and MLT on patient-derived organoids (PDOD). A. Chronological development of PDOD in Matrigel droplet. Organoid structures were confirmed using an inverted light microscope. B. PDOD were treated with or without AGP or MLT and morphology was assessed by light microscopy. C. FITC labeled anti-Ki-67 and DAPI staining of PDOD in the presence or absence of AGP or MLT evaluated by fluorescence microscopy.

Availability of data and materials

The datasets generated and analyzed during the current study are not publicly available due to continuing the research but are available from the corresponding author on reasonable request.

Authors' contributions

T.G.B., S.J.C., A.B. Conceptualization. A.BF providing the surgical tissues. N.S., T.I., E.H, S.G. performed the experiments and analyzed the data. N.S., and A.B. writing-original draft

preparation, T.G.B., and S.J.C., A.BF reviewing and editing. A.B. supervision. All authors have read and approved the final manuscript.

Patient consent for publication

Not applicable.

Ethics approval and consent to participate

University of Maryland Institutional Review Board (HP-00066889-3)

Competing interests

This study has been the subject of a patent application by TGB, SJC, and AB of the University of Maryland School of Medicine. The current status of the application is pending.

References

1. Society AC. Survival Rates for Colorectal Cancer. 2020; <https://www.cancer.org/cancer/colon-rectal-cancer/detection-diagnosis-staging/survival-rates.html>, 2020.
2. Chapuis PH, Bokey E, Chan C, et al. Recurrence and cancer-specific death after adjuvant chemotherapy for Stage III colon cancer. *Colorectal Dis*. 2019;21(2):164-173.
3. Dienstmann R, Salazar R, Tabernero J. Personalizing colon cancer adjuvant therapy: selecting optimal treatments for individual patients. *J Clin Oncol*. 2015;33(16):1787-1796.
4. Hodgkinson N, Kruger CA, Abrahamse H. Targeted photodynamic therapy as potential treatment modality for the eradication of colon cancer and colon cancer stem cells. *Tumour Biol*. 2017;39(10):1010428317734691.

1
2
3 1 5. Bayat Mokhtari R, Homayouni TS, Baluch N, et al. Combination therapy in combating
4
5 2 cancer. *Oncotarget*. 2017;8(23):38022-38043.
6
7
8 3 6. Wang Z, Wei Y, Fang G, et al. Colorectal cancer combination therapy using drug and gene
9
10 4 co-delivered, targeted poly(ethylene glycol)-epsilon-poly(caprolactone) nanocarriers.
11
12 5 *Drug Des Devel Ther*. 2018;12:3171-3180.
13
14
15 6 7. Banerjee A, Ahmed H, Yang P, Czinn SJ, Blanchard TG. Endoplasmic reticulum stress
16
17 7 and IRE-1 signaling cause apoptosis in colon cancer cells in response to andrographolide
18
19 8 treatment. *Oncotarget*. 2016;7(27):41432-41444.
20
21
22 9 8. Banerjee A, Banerjee V, Czinn S, Blanchard T. Increased reactive oxygen species levels
23
24 10 cause ER stress and cytotoxicity in andrographolide treated colon cancer cells. *Oncotarget*.
25
26 11 2017;8(16):26142-26153.
27
28
29 12 9. Blanchard TG, Lapidus R, Banerjee V, et al. Upregulation of RASSF1A in Colon Cancer
30
31 13 by Suppression of Angiogenesis Signaling and Akt Activation. *Cell Physiol Biochem*.
32
33 14 2018;48(3):1259-1273.
34
35
36 15 10. Islam MT, Ali ES, Uddin SJ, et al. Andrographolide, a diterpene lactone from
37
38 16 Andrographis paniculata and its therapeutic promises in cancer. *Cancer Lett*.
39
40 17 2018;420:129-145.
41
42
43 18 11. Wang W, Guo W, Li L, et al. Andrographolide reversed 5-FU resistance in human
44
45 19 colorectal cancer by elevating BAX expression. *Biochem Pharmacol*. 2016;121:8-17.
46
47
48 20 12. Akbarzadeh M, Movassaghpour AA, Ghanbari H, et al. The potential therapeutic effect of
49
50 21 melatonin on human ovarian cancer by inhibition of invasion and migration of cancer stem
51
52 22 cells. *Sci Rep*. 2017;7(1):17062.
53
54
55
56
57
58
59
60

13. Hao J, Fan W, Li Y, et al. Melatonin synergizes BRAF-targeting agent vemurafenib in melanoma treatment by inhibiting iNOS/hTERT signaling and cancer-stem cell traits. *J Exp Clin Cancer Res.* 2019;38(1):48.
14. Su SC, Hsieh MJ, Yang WE, Chung WH, Reiter RJ, Yang SF. Cancer metastasis: Mechanisms of inhibition by melatonin. *J Pineal Res.* 2017;62(1).
15. Gil-Martin E, Egea J, Reiter RJ, Romero A. The emergence of melatonin in oncology: Focus on colorectal cancer. *Med Res Rev.* 2019;39(6):2239-2285.
16. Buldak RJ, Pilc-Gumula K, Buldak L, et al. Effects of ghrelin, leptin and melatonin on the levels of reactive oxygen species, antioxidant enzyme activity and viability of the HCT 116 human colorectal carcinoma cell line. *Mol Med Rep.* 2015;12(2):2275-2282.
17. Lee JH, Yun CW, Han YS, et al. Melatonin and 5-fluorouracil co-suppress colon cancer stem cells by regulating cellular prion protein-Oct4 axis. *J Pineal Res.* 2018;65(4):e12519.
18. Banerjee A. Organoid culture and its importance. *Gastroenterology and Hepatology International Journal.* 2017;2(2):1-2.
19. Blanchard TG, Czinn SJ, Banerjee V, et al. Identification of Cross Talk between FoxM1 and RASSF1A as a Therapeutic Target of Colon Cancer. *Cancers (Basel).* 2019;11(2).
20. Banerjee A, Basu M, Blanchard TG, et al. Early Molecular Events in Murine Gastric Epithelial Cells Mediated by Helicobacter pylori CagA. *Helicobacter.* 2016;21(5):395-404.
21. Wiener Z, Band AM, Kallio P, et al. Oncogenic mutations in intestinal adenomas regulate Bim-mediated apoptosis induced by TGF-beta. *Proc Natl Acad Sci U S A.* 2014;111(21):E2229-2236.

1
2
3 1 22. Garcia-Navarro A, Gonzalez-Puga C, Escames G, et al. Cellular mechanisms involved in
4
5 2 the melatonin inhibition of HT-29 human colon cancer cell proliferation in culture. *J Pineal*
6
7 *Res.* 2007;43(2):195-205.
8
9
10 4 23. Liu Z, Zou D, Yang X, et al. Melatonin inhibits colon cancer RKO cell migration by
11
12 5 downregulating Rhoassociated protein kinase expression via the p38/MAPK signaling
13
14 6 pathway. *Mol Med Rep.* 2017;16(6):9383-9392.
15
16
17 7 24. Kim H, Lee GR, Kim J, et al. Sulfiredoxin inhibitor induces preferential death of cancer
18
19 8 cells through reactive oxygen species-mediated mitochondrial damage. *Free Radic Biol*
20
21 9 *Med.* 2016;91:264-274.
22
23
24 10 25. Lin F, Zhang P, Zuo Z, et al. Thioredoxin-1 promotes colorectal cancer invasion and
25
26 11 metastasis through crosstalk with S100P. *Cancer Lett.* 2017;401:1-10.
27
28 12 26. Raffel J, Bhattacharyya AK, Gallegos A, et al. Increased expression of thioredoxin-1 in
29
30 13 human colorectal cancer is associated with decreased patient survival. *J Lab Clin Med.*
31
32 14 2003;142(1):46-51.
33
34
35 15 27. Dekker E, Tanis PJ, Vleugels JLA, Kasi PM, Wallace MB. Colorectal cancer. *Lancet.*
36
37 16 2019;394(10207):1467-1480.
38
39
40 17 28. Xie YH, Chen YX, Fang JY. Comprehensive review of targeted therapy for colorectal
41
42 18 cancer. *Signal Transduct Target Ther.* 2020;5(1):22.
43
44
45 19 29. Siegel RL, Miller KD, Jemal A. Cancer statistics, 2019. *CA Cancer J Clin.* 2019;69(1):7-
46
47 20 34.
48
49 21 30. Khan I, Mahfooz S, Ansari IA. Antiproliferative and Apoptotic Properties of
50
51 22 Andrographolide Against Human Colon Cancer DLD1 Cell Line. *Endocr Metab Immune*
52
53 *Disord Drug Targets.* 2020;20(6):930-942.
54
55
56
57
58
59
60

- 1
2
3 1 31. Yang L, Wu D, Luo K, Wu S, Wu P. Andrographolide enhances 5-fluorouracil-induced
4
5 2 apoptosis via caspase-8-dependent mitochondrial pathway involving p53 participation in
6
7 3 hepatocellular carcinoma (SMMC-7721) cells. *Cancer Lett.* 2009;276(2):180-188.
8
9
10 4 32. Lin HH, Shi MD, Tseng HC, Chen JH. Andrographolide sensitizes the cytotoxicity of
11
12 5 human colorectal carcinoma cells toward cisplatin via enhancing apoptosis pathways in
13
14 6 vitro and in vivo. *Toxicol Sci.* 2014;139(1):108-120.
15
16
17 7 33. Su M, Qin B, Liu F, Chen Y, Zhang R. Andrographolide enhanced 5-fluorouracil-induced
18
19 8 antitumor effect in colorectal cancer via inhibition of c-MET pathway. *Drug Des Devel*
20
21 9 *Ther.* 2017;11:3333-3341.
22
23
24 10 34. Banerjee V, Sharda N, Huse J, et al. Synergistic potential of dual andrographolide and
25
26 11 melatonin targeting of metastatic colon cancer cells: Using the Chou-Talalay combination
27
28 12 index method. *Eur J Pharmacol.* 2021;897:173919.
29
30
31 13 35. Reiter RJ, Rosales-Corral SA, Tan DX, et al. Melatonin, a Full Service Anti-Cancer Agent:
32
33 14 Inhibition of Initiation, Progression and Metastasis. *Int J Mol Sci.* 2017;18(4).
34
35 15 36. Reiter RJ, Sharma R, Ma Q, Rosales-Corral S, de Almeida Chuffa LG. Melatonin inhibits
36
37 16 Warburg-dependent cancer by redirecting glucose oxidation to the mitochondria: a
38
39 17 mechanistic hypothesis. *Cell Mol Life Sci.* 2020.
40
41
42 18 37. Banerjee A, Czinn SJ, Reiter RJ, Blanchard TG. Crosstalk between endoplasmic reticulum
43
44 19 stress and anti-viral activities: A novel therapeutic target for COVID-19. *Life Sci.*
45
46 20 2020;255:117842.
47
48
49 21 38. Fic M, Gomulkiewicz A, Grzegorzolka J, et al. The Impact of Melatonin on Colon Cancer
50
51 22 Cells' Resistance to Doxorubicin in an in Vitro Study. *Int J Mol Sci.* 2017;18(7).
52
53
54
55
56
57
58
59
60

1
2
3 1 39. Romero A, Egea J, Garcia AG, Lopez MG. Synergistic neuroprotective effect of combined
4
5 2 low concentrations of galantamine and melatonin against oxidative stress in SH-SY5Y
6
7 3 neuroblastoma cells. *J Pineal Res.* 2010;49(2):141-148.
8
9
10 4 40. Majumder D NP, Debnath R, Maiti D. Understanding the complicated relationship between
11
12 5 antioxidants and carcinogenesis. *J Biochem Mol Toxicol.* 2020(Sep 29).
13
14
15 6 41. Kim YJ, Ahn JY, Liang P, Ip C, Zhang Y, Park YM. Human prx1 gene is a target of Nrf2
16
17 7 and is up-regulated by hypoxia/reoxygenation: implication to tumor biology. *Cancer Res.*
18
19 8 2007;67(2):546-554.
20
21
22 9 42. Grassi L, Alfonsi R, Francescangeli F, et al. Organoids as a new model for improving
23
24 10 regenerative medicine and cancer personalized therapy in renal diseases. *Cell Death Dis.*
25
26 11 2019;10(3):201.
27
28
29 12 43. Li FY, Wu SG, Zhou J, et al. Prognostic value of Ki-67 in breast cancer patients with
30
31 13 positive axillary lymph nodes: a retrospective cohort study. *PLoS One.* 2014;9(2):e87264.
32
33
34 14 44. Cidado J, Wong HY, Rosen DM, et al. Ki-67 is required for maintenance of cancer stem
35
36 15 cells but not cell proliferation. *Oncotarget.* 2016;7(5):6281-6293.
37
38
39 16
40
41
42
43
44
45
46
47
48
49
50
51
52
53
54
55
56
57
58
59
60

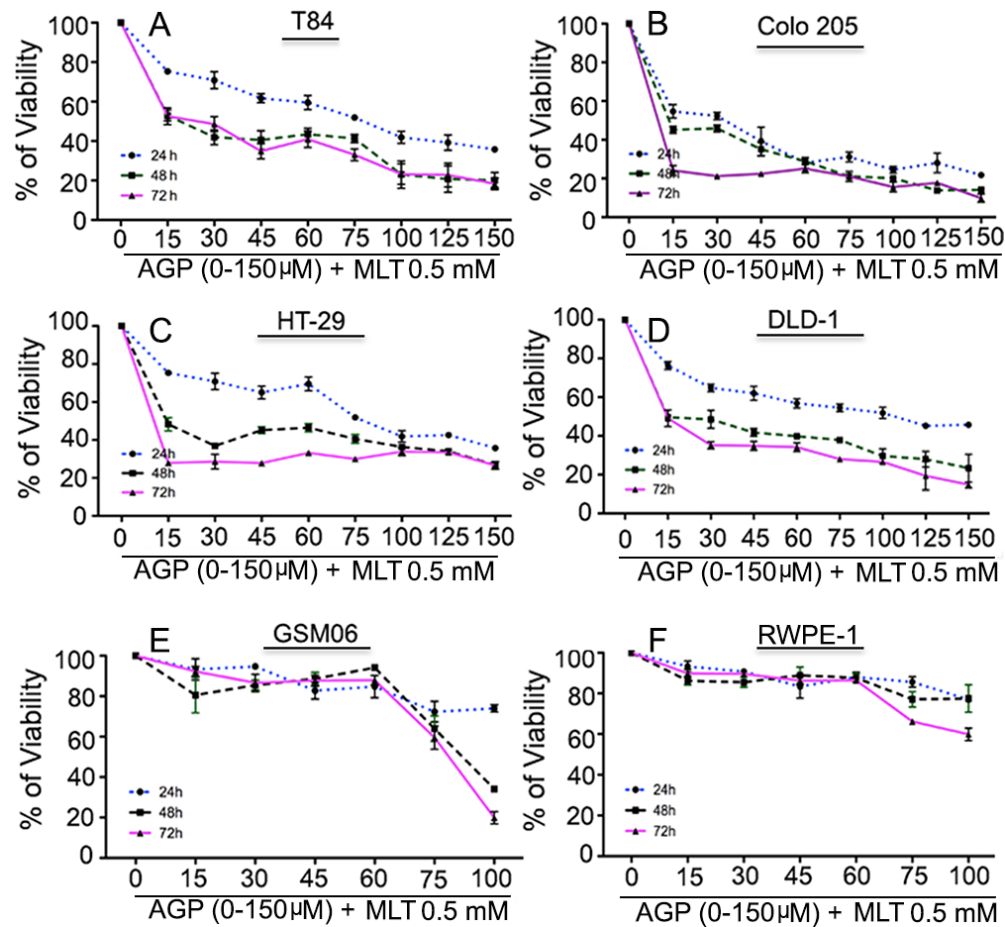


Figure 1. Impact of AGP and MLT on mCRC cell viability.

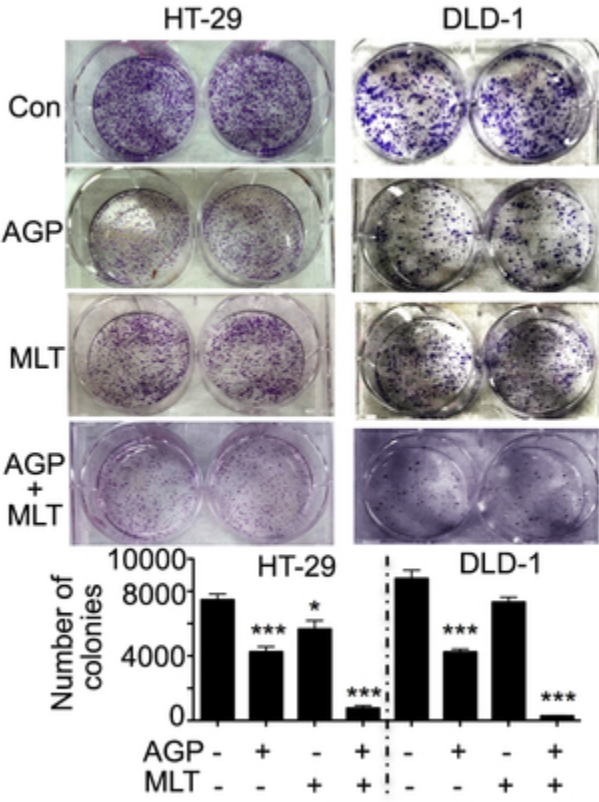


Figure 2. Co-treatment suppress clonogenicity in HT-29 and DLD-1 cells.

26x33mm (300 x 300 DPI)

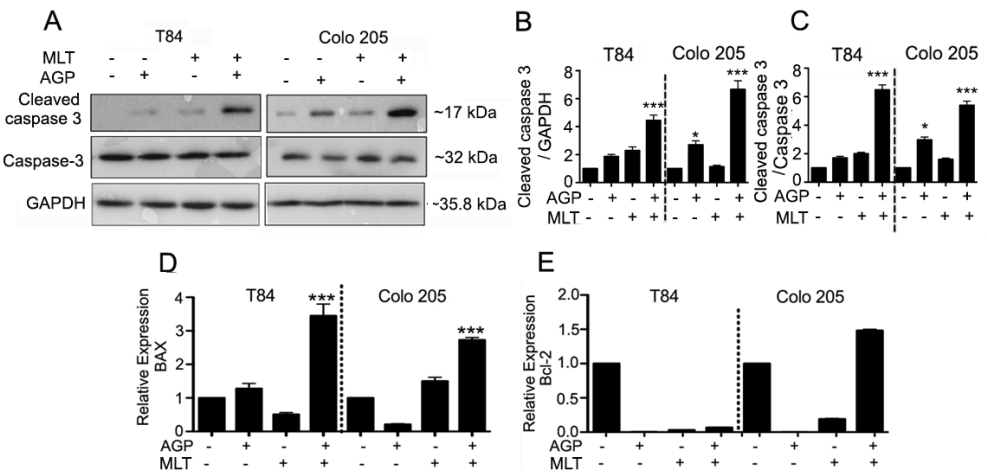


Figure 3. Co-treatment of AGP and MLT induced cell apoptosis.

1
2
3
4
5
6
7
8
9
10
11
12
13
14
15
16
17
18
19
20
21
22
23
24
25
26
27
28
29
30
31
32
33
34
35
36
37
38
39
40
41
42
43
44
45
46
47
48
49
50
51
52
53
54
55
56
57
58
59
60

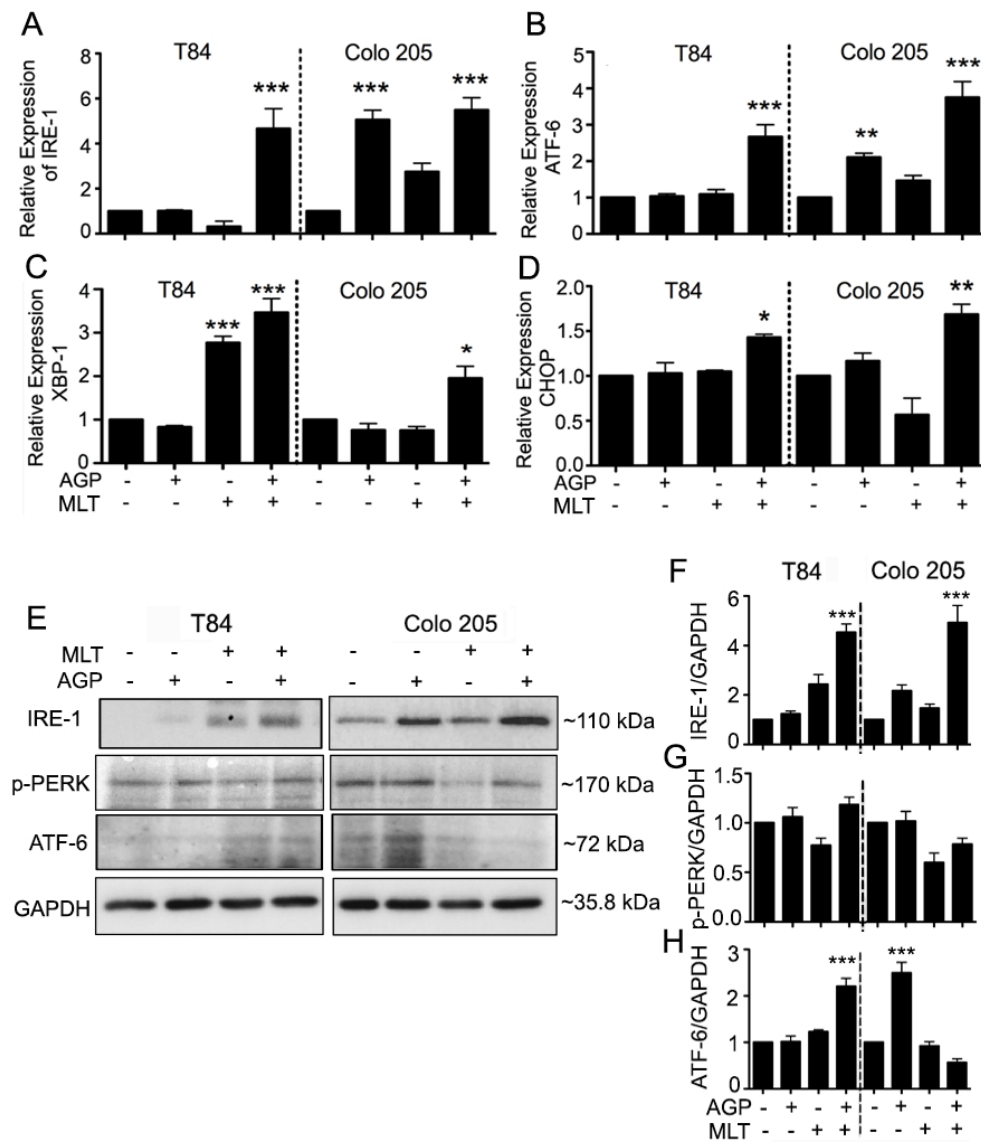


Figure 4. AGP and MLT induces ER stress-related IRE-1 and associated proteins.

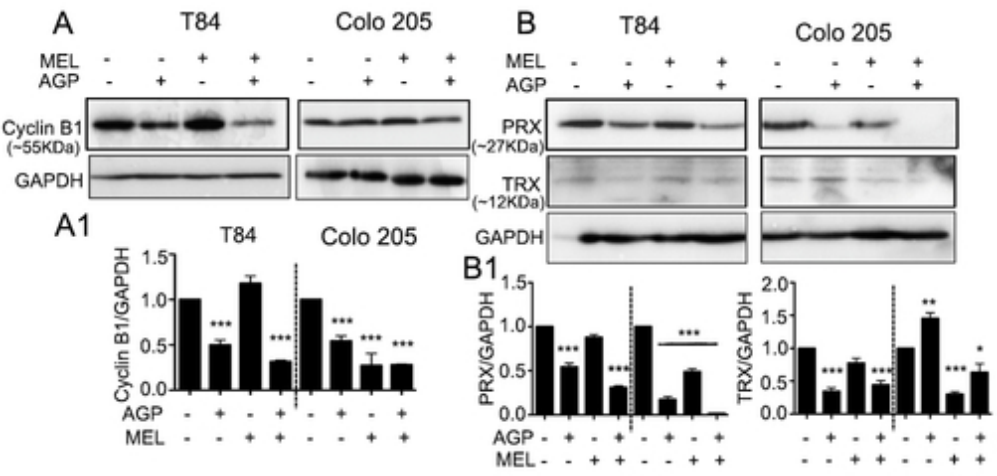


Figure 5. Co-treatment induced cell cycle arrest and decreased antioxidant protein expression in CRC cells.

42x20mm (300 x 300 DPI)

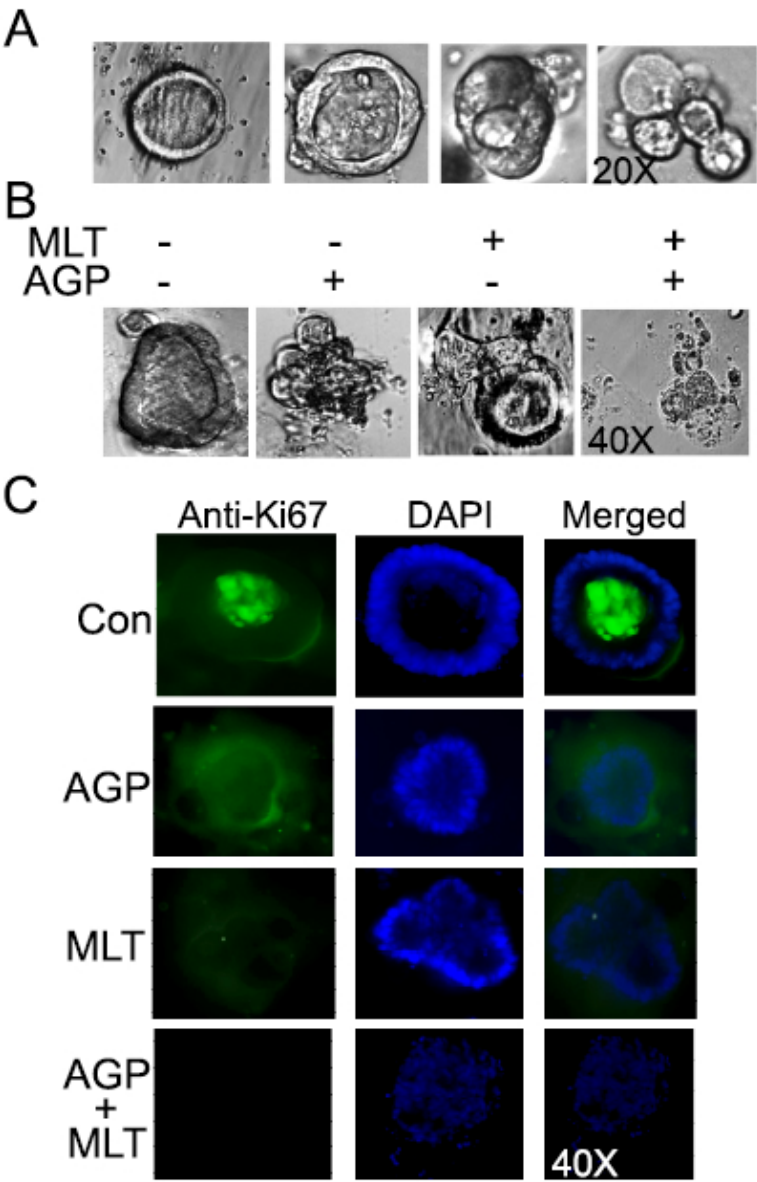


Figure 6. Impact of AGP and MLT on patient-derived organoids (PDOD).

Supplementary Table-1: qRT-PCR primers

Gene	Primer sequence forward	Primer sequence reverse
GAPDH	5'-CGACCACTTTGTCAAGCTCA-3'	5'-AGGGGAGATTCAGTGTGGTG-3'
IRE-1	5'-GGGAAATACTCTACCAGCCT-3'	5'-GAAATCTCTCCAGCATCTTG-3'
ATF6	5'-TCAGGGAGTGAGCTACAAGT-3'	5'-CTTGTGGTCTTGTTATGGGT-3'
CHOP	5'-TTCTCTGGCTTGGCTGACTG-3'	5'-CTGCGTATGTGGGATTGAGG-3'
Bcl-2	5'-GGAGGCTGGGATGCCTTT3'	5'-ACCCATGGCGGTGACCATGC-3'
Bax	5'-GAGAGGTCTTTTTCCGAGTGG-3'	5'-CCTTGAGCACCAGTTTGCTG-3'
XBP1	5'-AACCAGGAGTTAAGACAGCGCTT-3'	5'-CTGCACCCTCTGCGGACT-3'